A detailed study of the site of Mg-halo as detected by CMA

Dr. Haruki Itofuji*†
†Technical Development Section Ube Steel Co., Ltd. 1978-19 Okinoyama, Kogushi, Ube City Yamaguchi Pref., 755-0067 Japan

A detailed study of magnesium distribution in the microstructure of spheroidal graphite iron was conducted using a Computer Aided Micro Analyzer (CMA). The results showed that magnesium segregated in a halo-like form at the site between the eutectic graphite core and the secondary graphite ring in graphite nodules. The graphite ring was in the form of a three-dimensional graphite shell. The halo-like distribution was concluded to be the trace of a magnesium gas bubble. In this study, the Site Theory has been used as one means of interpreting the data. According to the Site Theory, a magnesium gas bubble in liquid iron functions as the site for the nucleation and growth of spheroidal graphite. Other interpretations of the presented data are welcomed.

Keywords: site theory, Mg-halo, CMA, spheroidal graphite iron, gas bubble.

Introduction

In a previous study[1] of spheroidal graphite structure in ductile iron, a magnesium halo was found around the graphite nodule. The magnesium halo consisted of metallic magnesium, according to CMA analysis. For the purposes of this paper, metallic magnesium is defined as free magnesium. A good relationship between free magnesium and graphite nodularity has already been verified.[2] However, the detailed location of the magnesium halo in the graphite nodule has not been verified, due to low analysis magnification. Considering the solubility of magnesium in austenite, and the growth behaviour of secondary graphite, the location of the magnesium halo was predicted to exist at the site between the eutectic graphite core and secondarily precipitated graphite ring.[3,4,5] This study aims to find the distinct magnesium halo in a graphite nodule by high magnification analysis. The findings have also been interpreted in relation to the Site Theory of the nucleation and growth behaviour of spheroidal graphite and other types of graphite in liquid and solid state of irons.[1–10]

Experimental procedure

An as-cast specimen, 15 mm × 15 mm × 10 mm taken from a heavy section test block (thickness = 150 mm) was used for the CMA analysis in this study. This was the same specimen used in previous studies.[1,3,4,5] The chemical composition is shown in Table 1. To check the influence of polishing on the analytical result, the CMA analyses were conducted on two different surface conditions. One was a surface polished with diamond paste. The other was a surface milled by the glow discharge method. In these analyses, the same area in a specimen, but different layers, were analysed each time. To find the precise location of the magnesium halo in spheroidal graphite, a higher magnification was used than in the previous studies.[1,3,4,5] The analyses and discharge conditions are shown in Table 2 and 3 respectively.

Results

The microstructures analysed through CMA analyses are shown in Fig. 1. To avoid the influence of etchant, the microstructure in Fig. 1a was etched with 3% Nital after the first analysis. The unetched area is equal to the analysed area. It is generally known that the area bombarded by electrons is not etched, because of the carbon-deposited membrane. The results of the first analysis are shown in Fig. 2. The magnesium halo was observed at a layer slightly in from the surface, in most of the graphite nodules (Fig. 2a). This is obviously seen in the magnesium-iron combined map in Fig. 2c. Magnesium segregated almost at the centre, in some graphite nodules, but such nodules also had the magnesium halo. There was irregular graphite without the magnesium halo (seen at the right hand bottom corner in Fig. 1). It was, however, considered that this nodule exposed a surface layer of spheroidal graphite and such a layer was outside the magnesium halo. A Vickers hardness indentation mark was intentionally taken in the analysis area to show the typical noise phenomena in this kind of analysis. The detector for the sphecial X-ray caused by the electron

Table 1 Chemical composition of specimen for CMA analysis

Chemical composition (mass%)						
C	Si	Mn	P	S	Mg	CE
3.53	2.31	0.27	0.037	0.010	0.051	4.30

CE = C + 1/3Si

*Author for correspondence.
e-mail: h-itofuji@mx5.tiki.ne.jp

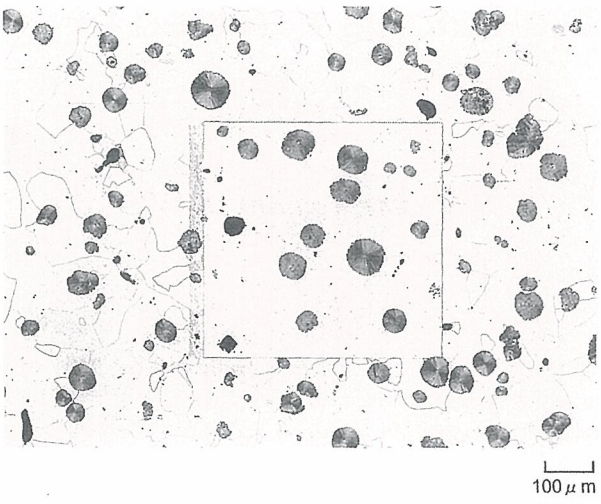

Fig. 1 Microstructure of a hand-polished specimen analysed by CMA; (a) optical photo and (b) SEM photo. The specimen was etched with 3% Nital after analysis

irradiation in CMA was on the upper side of the analysis area in Fig. 1. The result showed that noise was detected on the upper half, at the slope of the pyramidal hole, as shown in the bottom left hand corner of Fig. 2. If CMA detected noise from the special X-ray on the graphite surface, the analysis result would indicate the directional magnesium map, as with the hardness indentation mark. Magnesium was, however, detected as a ringed segregation in the graphite nodules. The map had no directionality from the detector. This proves that magnesium segregated in a halo-like form in graphite nodules.

Magnesium was also enriched at voids and inclusions. The SEM photographs of void and typical inclusions are shown in Fig. 3 and 4 respectively. The small black spots in Fig. 1a and the white spots in Fig. 1b are magnesium-contained inclusions. A little magnesium segregation among the eutectic cells was observed, as found in the last study.[1,3] (Fig. 2c)

The second analysis was carried out on the other surface layer as shown in Fig. 5. The results of the second analysis are shown in Fig. 6. A different type of CMA was used for this analysis, and therefore the expression of the data is a little different. The magnesium halo was also detected on most graphite nodules, just as in the first analysis. This means that polishing has almost no influence on the result of CMA analysis. A carbon-deficient ring was detected in some graphite nodules, as shown in Fig. 6b. The magnesium halo was located at the same site as the carbon-deficient ring. The ring might be the interfacial site between primary and secondary graphite. The distribution of argon was detected in most graphite nodules, as shown in Fig. 6(c). The degree of segregation was especially strong at the same position as the magnesium halo. The argon segregation might occur during glow discharge spattering. These questions will be made clear later in this paper. Magnesium was detected at the centre of some graphite nodules in greater numbers than in the first analysis. Those nodules also had the magnesium halo. The SEM photographs of such nodules are shown in Fig. 7, for example. The degree of milling by the glow discharging method was different between the centre and the periphery area in graphite nodules. The degree of milling at the centre area was less than that at the periphery. It seemed that this tendency came from the different milling behaviour between the basal plane and the prism face in the hexagonal graphite crystal structure. The substructure of spheroidal graphite has already been explained by the author.[3,4,7] Spheroidal graphite consists

Table 2 Conditions of CMA analysis on magnesium

Type of CMA	JEOL-8600M	Shimazu-8705
Accelerating voltage (KV)	15	15
Probe current (nA)	300	30
Beam diameter (mm)	1	1
Analysis region/beam[11] (μm)	$\phi 2 \times$ Depth 1	$\phi 2 \times$ Depth 1
Scanning (μm)	1 [Stage]	1 [Stage]
Points (x, y)	450×450	512×512
Dwell time (m-sec.)	100	100
Method	WDS	WDS
Standard specimen	MgO	Mg
Spectrum crystal	TAP	RAP
Surface preparation	Diamond polish (no etch)	Glow discharge spattering

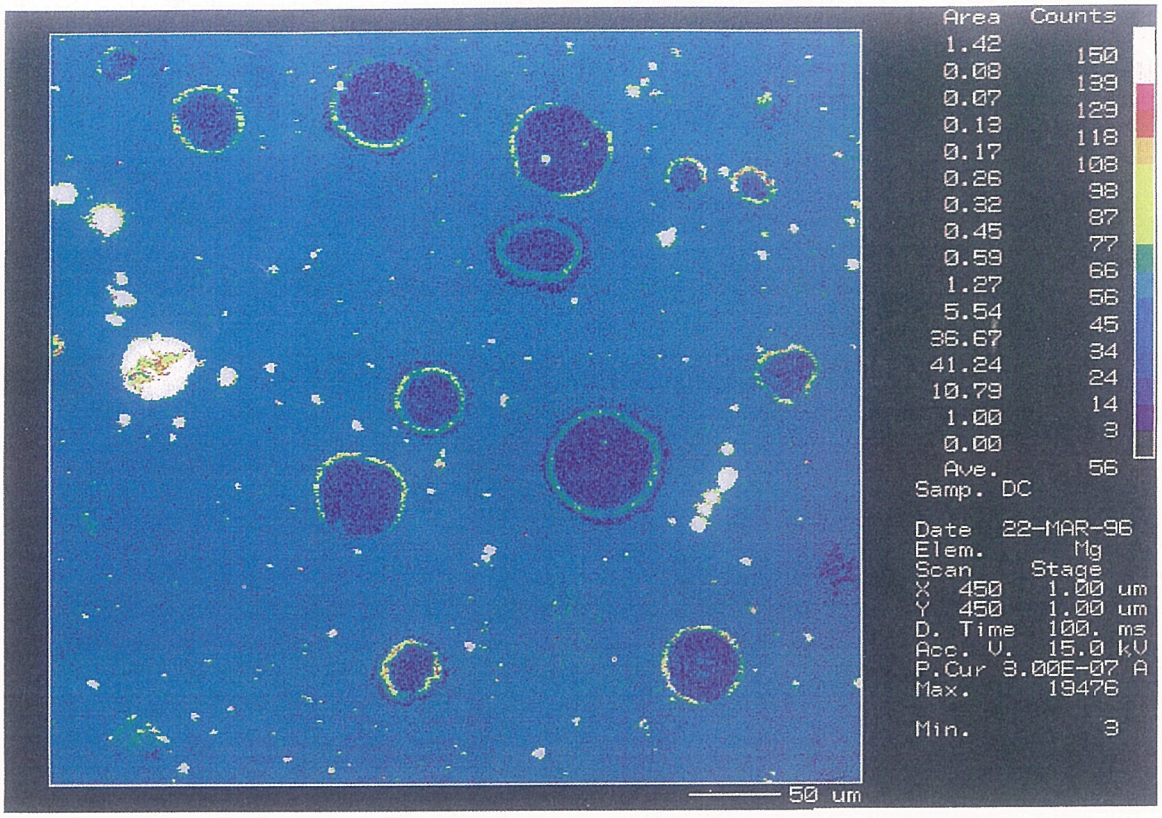

(a) Mg map

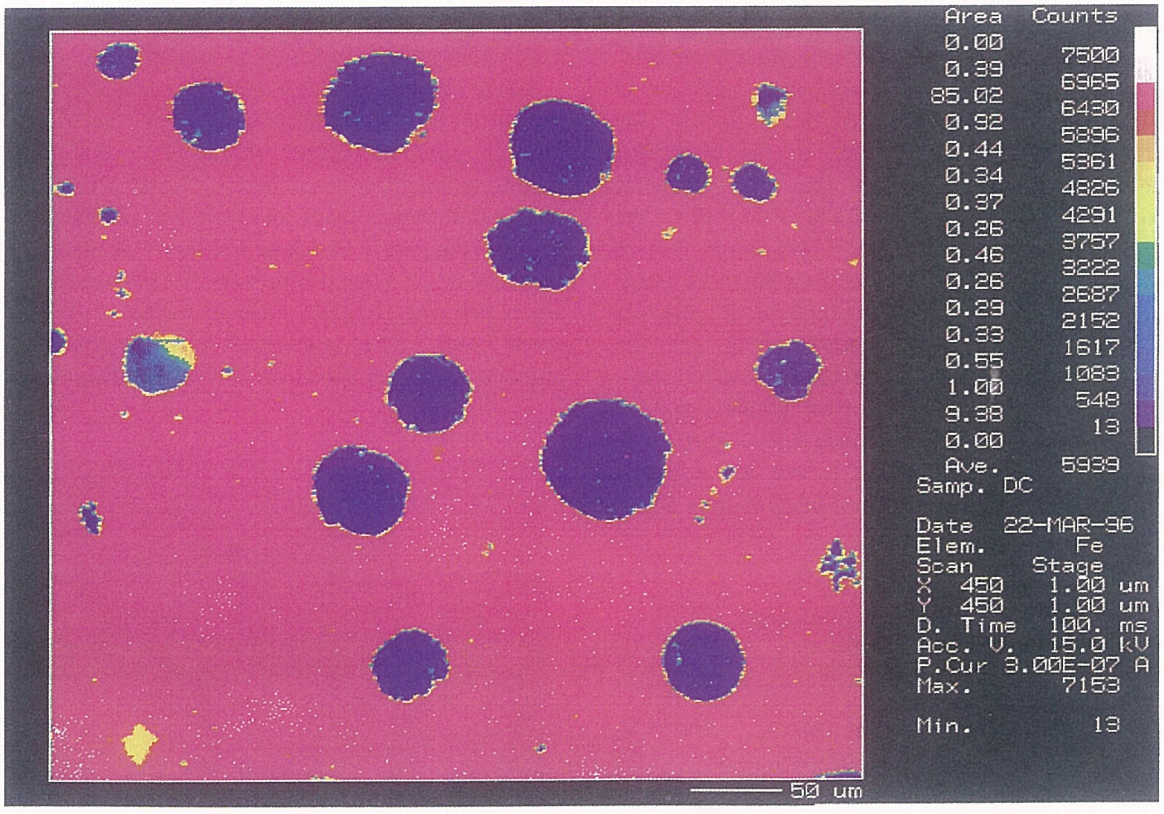

(b) Fe map

Fig. 2 The results of the CMA analysis of microstructure shown in Fig. 1

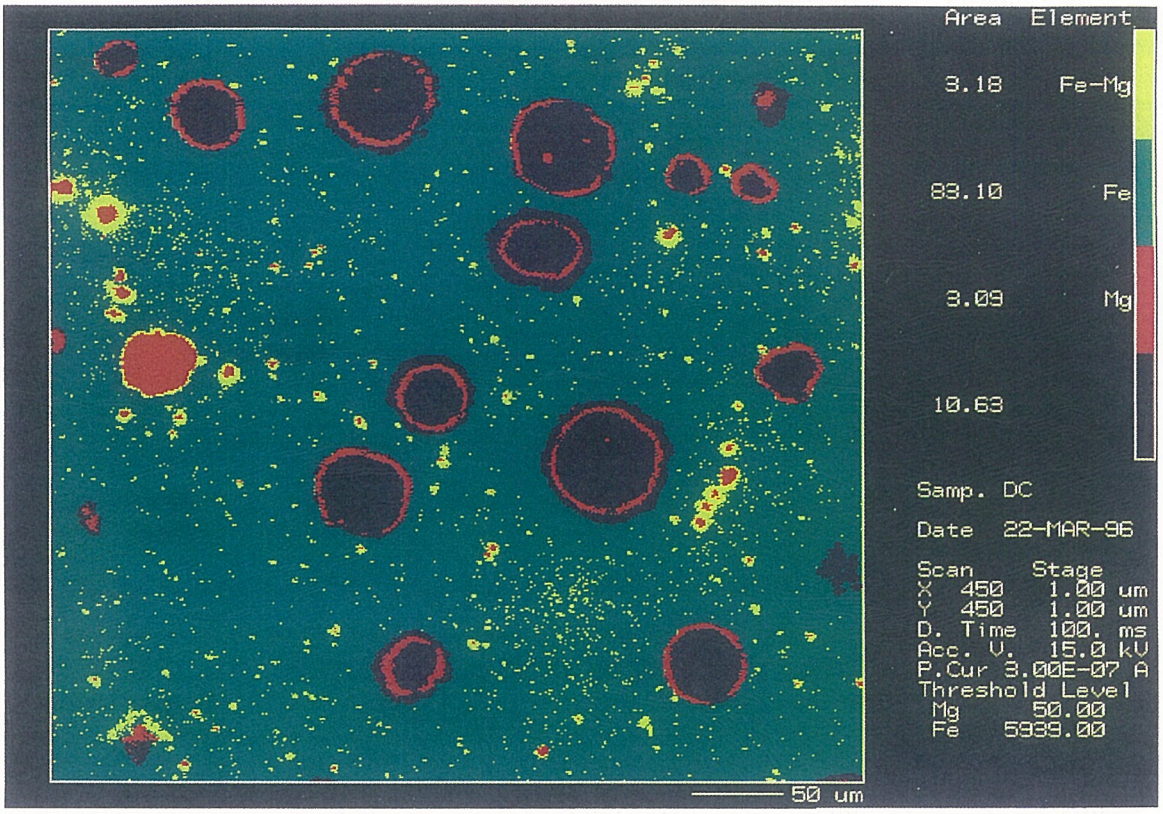

(c) Fe-Mg map

Fig. 2 *continued*

of thin graphite chips. The graphite chips build up in layers parallel to the surface of spheroidal graphite. The chip's face forms the basal plane of the hexagonal graphite crystal structure. When the basal plane is exposed at the polished surface, it is hard to mill on the surface. On the other hand, when the prism face is exposed on the milling surface, milling becomes much easier. If the above crystal substructure of the graphite nodule[3,4,7] is considered, it becomes clear that the exposure of the basal plane at the centre is much more likely than that at the periphery of the graphite nodule. Thus, it is certain that the protuberance at the centre of the graphite nodules as seen in Fig. 5 was the result of milling. The protuberance was not a nucleus-type object but rather layers of graphite chips.

Table 3 Conditions of glow discharge spattering by GD/MS

	For CMA	For SEM
Mask diameter (ϕ mm)	5	5
Insulator (ϕ mm)	5+20	5+20
Voltage (KV)	0.7	0.7
Current (mA)	1	1
Time (Min.)	50	140
Milling Depth (μm)	$\doteqdot$2	$\doteqdot$7
Atmosphere	Ar	Ar

GD/MS: Glow Discharge Mass Spectrometry

Some graphite nodules had the carbon-deficient and argon-rich ring where the Mg halo was located. To clear up this question, deeper milling by glow discharge spattering was conducted. The specimen was a different one from that previously analysed, but was taken from a neighboring part in the same test block. A clearance was observed at the same position as the carbon-deficient and argon-rich ring after the polished surface was milled off about 7 μm. A SEM photograph of an example of such a graphite nodule is shown in Fig. 8. Finally, the surface

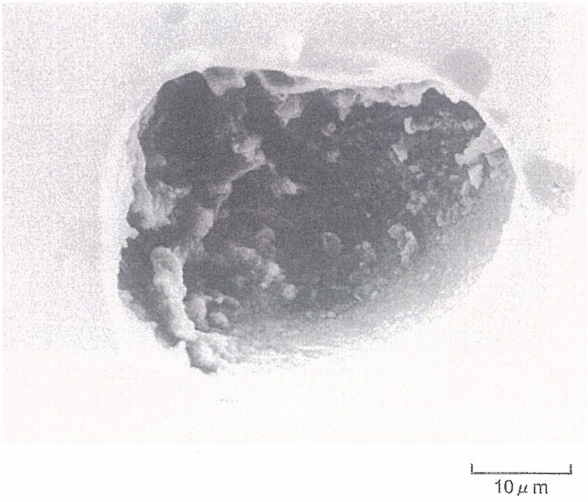

Fig. 3 The void at the left middle of the analysed area in Fig. 1

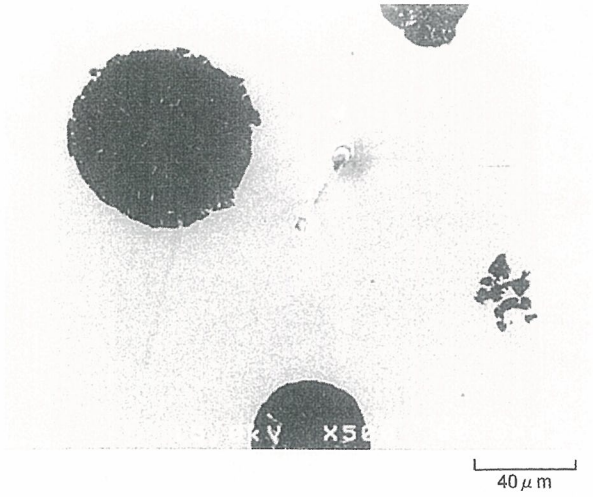

(a)

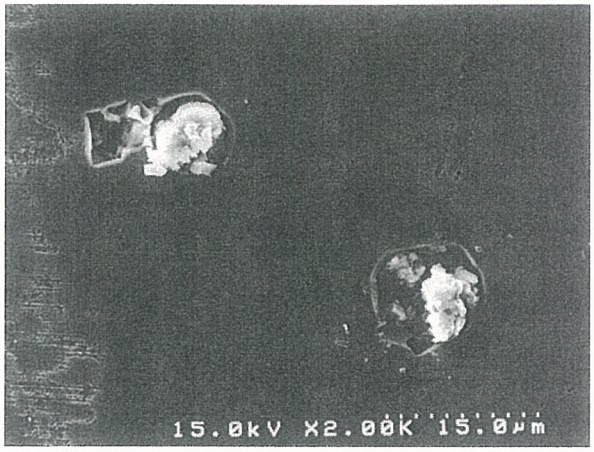

(b)

Fig. 4 Inclusions at the area among eutectic cells in Fig. 1; (a) the area at right middle and (b) the area at left upper

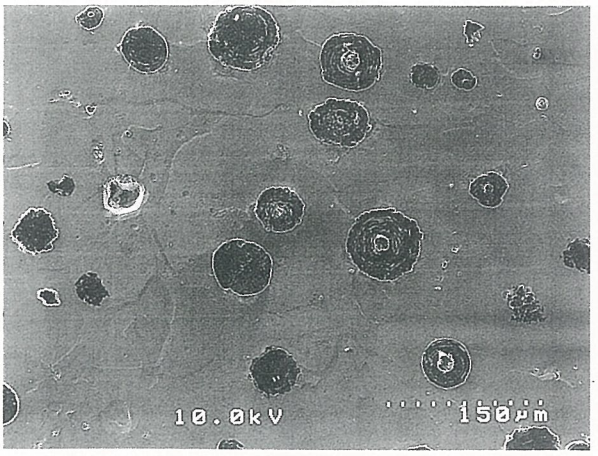

Fig. 5 SEM microstructure of a specimen which was used for the second CMA analysis. The analysed area was the same as the first CMA analysis, but the surface was milled about 2 μm by the glow discharge spattering method

layer of spheroidal graphite consisted of a graphite shell. A. Javaid, *et al.*[12] reported the same results. As they concluded, it is considered that the graphite shell has to be the secondary graphite. The outline of the secondary graphite shell is usually observed as a ring in a well-polished graphite nodule[5] when using optical microscopy. The secondary graphite shell was not a single crystal and was constructed from layers of thin graphite chips, the same as the core nodule. The protuberance was also observed at the centre area in graphite nodules this time. The top surface was the basal plane. The example is shown in Fig. 8.

Discussion

Magnesium is not only a spheroidizing element but also a strong desulphurizing and deoxidizing element for base iron. As already reported,[2] magnesium exists as two morphologies in treated iron. One is inclusive magnesium such as a sulphide, an oxide etc. The other is free magnesium, which influences the graphite nodularity. Since free magnesium has almost no solubility in liquid iron,[13] and vaporises above about 1100°C under one atmosphere pressure, it is necessarily in a gaseous state and exists as a gas bubble. In addition, the solubility of free magnesium in the austenite phase during and after solidification is much less than that in liquid iron. There is no existence of magnesium carbide over about 660°C.[14] From all of the above, if spheroidal graphite could nucleate and grow in the magnesium gas bubble, it would be easily predicted that magnesium had to be located at the site between spheroidal graphite and the matrix structure. This was already verified by locating a magnesium halo in previous studies.[1,3,4] The precise location of the magnesium halo could not, however, be distinguished at that time because of the low analysis magnification. Under the high analysis magnification used this time, the precise location of the magnesium halo in spheroidal graphite was verified to be at the site between the eutectic graphite core and secondary graphite ring (shell), just as predicted in previous papers.[3,4,5] One explanation of the formation process of the magnesium halo and its final location is the Site Theory.

The magnesium gas bubble may be considered as a kind of free surface in liquid iron for graphite precipitation. Graphite has the natural tendency to nucleate and grow dominantly at such a free surface.[15–17] According to the Site Theory, a magnesium gas bubble is an indispensably necessary condition for graphite to directly nucleate and form the spheroidal morphology in liquid iron. According to the theory, graphite forms into a sphere sphape within the magnesium gas bubble. The size is under 10 μm. The gassy magnesium halo might exist at the interfacial site between such sphere graphite and liquid iron at this stage of the solidification.

The austenite shell gradually surrounds the sphere graphite directly precipitated in liquid iron when the solidification progresses further. Sphere graphite within the austenite shell must be located away from the residual liquid iron to complete the spheroidal form. This means

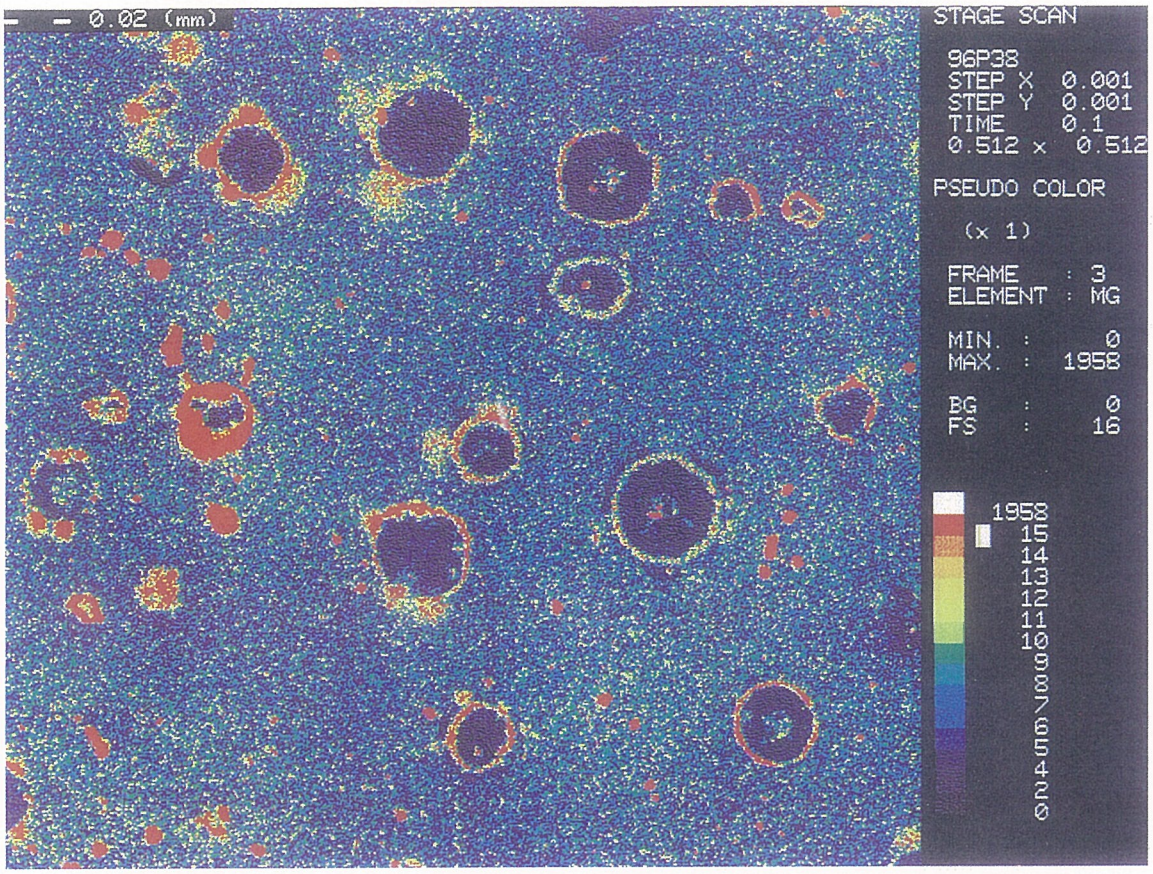

(a) Mg map

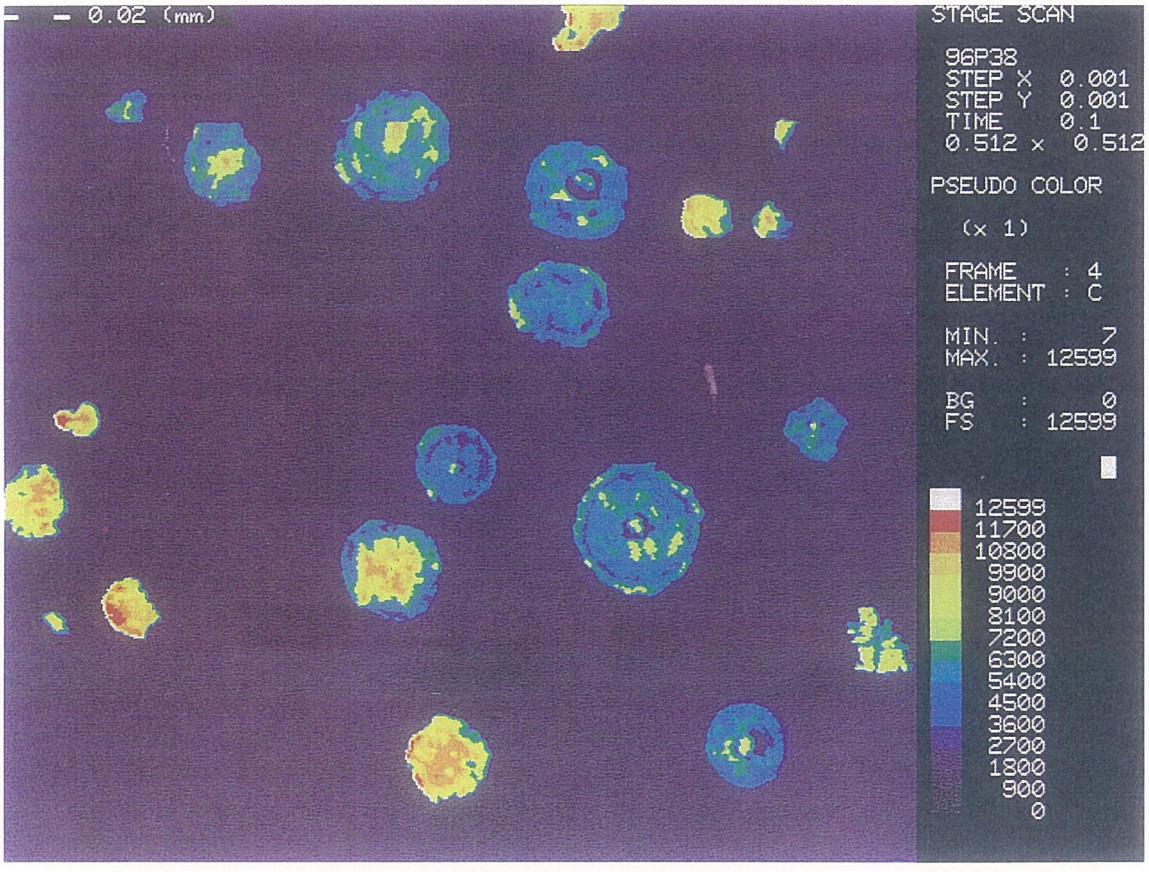

(b) C map

Fig. 6 The results of CMA analysis on the microstructure shown in Fig. 5

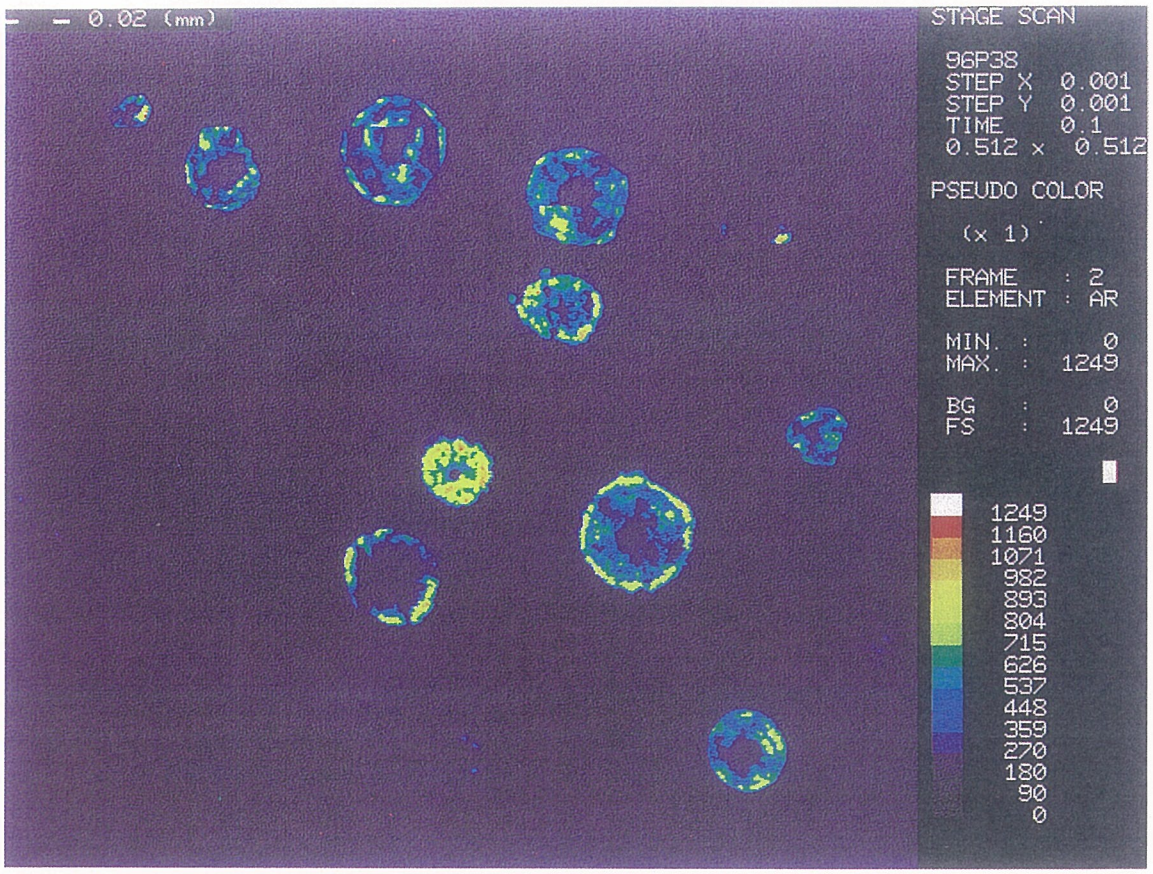

(c) Ar map

Fig. 6 *continued*

that the inside wall of the austenite shell facing the sphere graphite must exist in a round form. The shape depends on the behaviour of the liquid channel in austenite shell.[3,6] The round wall within the austenite shell is a sufficient condition for sphere graphite to grow the spheroidal morphology. The gassy magnesium halo might exist at the interfacial site between the spheroidal graphite and the austenite shell at the end of the solidification. Gaseous magnesium liquidises at about 1100°C with a reduction in volume. Therefore, a vacuum space might occur at such a site.

When expounding this theory, the final position of the magnesium halo depends on the nucleation and growth behaviour of secondary graphite. Secondary graphite would nucleate at the wall of the austenite matrix and grow inwards in the vacuum space. If the vacuum space did not have sufficient volume, secondary graphite would grow outwards accompanied by iron atom diffusion. In either case, the magnesium halo is sandwiched by the eutectic graphite core and secondary graphite shell. Since there is clearance between the core and the shell, the later growth behaviour described above would be predominant. Naturally, little or no carbon would be analytically detected at such clearance as shown in Fig. 6(b). It is considered that argon moved into the clearance during glow discharge spattering. It seems that argon also appeared between the basal planes at the periphery area of spheroidal graphite if the surface was sufficiently milled off by glow discharge spattering. The volumetric change of magnesium from gas to liquid and then to solid would create a wider clearance to some degree. Although there was irregular graphite, without the magnesium halo, such graphite was considered to be part of secondary graphite, as seen in Figs. 1, 4 and 5.

If the Site Theory is accepted, the following phenomena can also be understood;

1 Although graphite naturally grows to the kish morphology when it directly precipitates in liquid iron,[3,6] graphite in magnesium-treated liquid iron can take the spheroidal form because of the existence of the magnesium gas bubble.
2 Spheroidal graphite can also be obtained by adding S, Se, Te, Bi, Pb, N_2 and Ar, although greater numbers of graphite nodules are not expected.[15,16] Those elements can be in a gaseous state, and might exist as a gas bubble in liquid iron for a short time.
3 Spheroidal graphite can also be obtained as secondary graphite in malleable iron when spheroidal voids are introduced by a special tempering heat treatment.[16,17] Even flake graphite can have round ends when the iron matrix, facing the graphite end, is rounded by a special heat treatment.[18] These are similar phenomenon to the nucleation and growth of graphite in the liquid state.
4 The ceramic form filter is well known as a good tool to catch inclusions, but never reduces graphite nodularity.[19] This is the reason why free magnesium

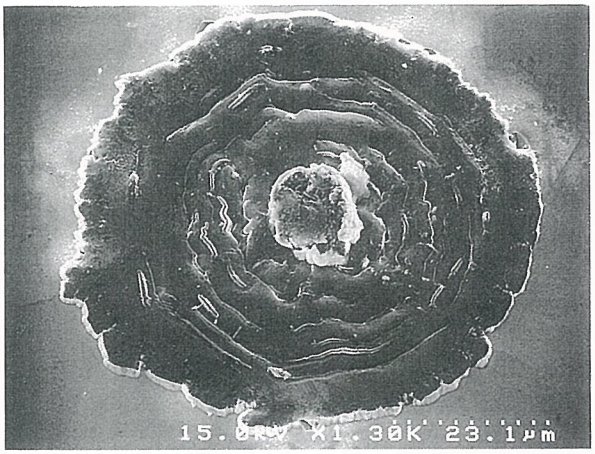

(a) Nodule with nucleous like protuberance at center

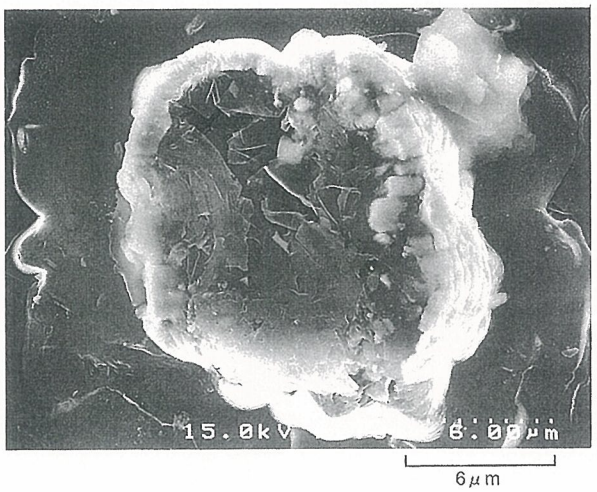

(b) High magnification of nucleous like protuberance

Fig. 7 SEM photographs of the largest graphite nodule at the near centre in Fig. 5 (tilted 30°). This nodule had a magnesium halo, but also had a magnesium-containing protuberance at the centre

contributes to graphite nodularity but inclusive magnesium does not.[2]

5 When magnesium-treated and non-treated liquid irons are poured into the same mould at the same time, the former always takes an upper layer position.[20] This is the reason why liquid iron with magnesium gas bubbles has a ligher density.

The role of magnesium on the formation of spheroidal graphite can be explained below. The graphite morphology depends on the site where graphite nucleates and grows. The special growth behaviour as influenced over the entire morphology never exists in spheroidal graphite. Even when graphite nodules have magnesium-contained inclusions at the centre, this is not an indispensable factor, since such nodules also have the magnesium halo.[1,3,4,5] The magnesium halo consists of metallic magnesium and must be the trace of a magnesium gas bubble. According to the Site Theory, a magnesium gas bubble provides the spheroidal site and indirectly contributes to the nucleation

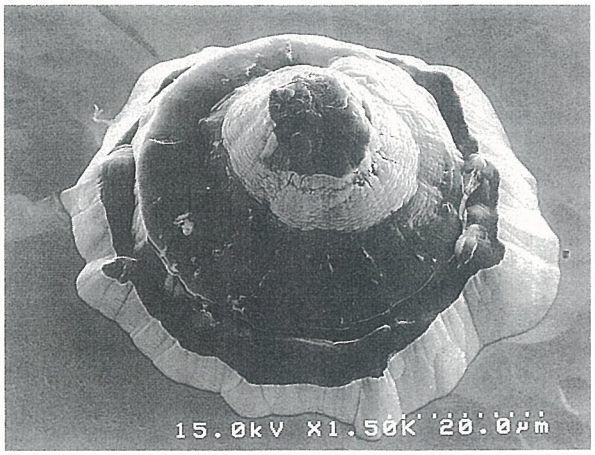

Fig. 8 SEM photograph of graphite nodule with secondary graphite ring (tilted 30°); the hand-polished surface was milled about 7 μm by glow discharge spattering

and growth of spheroidal graphite. Magnesium is the best element for spheroidal graphite formation in practical conditions. Locating the exact location of magnesium is in accordance with the Site Theory.

Conclusions

1 A magnesium halo was located at the site between the eutectic graphite nodule and the secondary graphite ring in most of the spheroidal graphite studied.
2 Magnesium segregated at the centre in some spheroidal graphite but such spheroidal graphite also had the magnesium halo.
3 The magnesium halo must be the trace of a magnesium gas bubble, and according to the Site Theory, this is where spheroidal graphite nucleates and grows.

Acknowledgment

I heartily thank Mr. Mark Fields of Cast-Fab Technologies, Inc. for his kind help in writing this paper. I wish to express appreciation to Miss Chiaki Takano for her kind support.

References

1. H. Itofuji, ''Magnesium Map of the Spheroidal Graphite Structure in Ductile Cast Irons'', *Cast Metals*, 1992, **5**, 1, 6–19.
2. H. Itofuji, ''The Influence of Free Magnesium on Some Properties in Spheroidal Graphite Irons'', *Int. J. Cast Metals Res.*, 1999, **12**, 179–187.
3. H. Itofuji, ''*Study on Graphite Spheroidization in Cast Irons*'', The Thesis of Doctor's Degree in Kyoto University, 1993.
4. H. Itofuji, ''Proposal of the Site Theory'', *AFS Trans.*, 1996, **104**, 79–87.
5. H. Itofuji, ''Letter to the Editor/Magnesium Map of the Spheroidal Graphite Structure in Ductile Cast Irons'', *Cast Metals*, 1993, **5**, 4, 235–237.

6. H. Itofuji, *et al.*, ''The Formation Mechanism of Compacted/vermicular Graphite in Cast Irons'', *AFS Trans.*, 1983, **91**, 831–840.
7. H. Itofuji, *et al.*, ''Comparison of Substructure of Compacted/vermicular Graphite with Other Types of Graphite'', *AFS Trans.*, 1983, **91**, 313–324.
8. H. Itofuji, *et al.*, ''Production and Evaluation of Heavy Section Ductile Cast Iron'', *AFS Trans.*, 1990, **98**, 585–595.
9. H. Itofuji, *et al.*, ''Formation Mechanism of Chunky Graphite in Heavy Section Ductile Cast Irons'', *AFS Trans.*, 1990, **98**, 429–448.
10. H. Itofuji, ''*Application of the Site Theory on the Quality Control of Heavy Section Spheroidal Graphite Cast Iron*'', Keith D. Millis World Symposium on Ductile Iron, Hilton Head Is., SC, Oct. 19–22, 1993.
11. R. Castaing, ''Electron Probe Microanalysis'', *Advance in Electronics and Electron Physics*, 1960, **13**, 317–386.
12. A. Javaid and C. R. Loper, Jr., ''Solid Graphitisation in Normalised and Annealed Ductile Cast Irons'', *AFS Trans.*, 1990, **98**, 597–608.
13. T. B. Massalski, *et al.*, ''Binary Alloy Phase Diagrams'', *ASM International*, 1992, 1722–1723.
14. T. B. Massalski, *et al.*, ''Binary Alloy Phase Diagrams'', *ASM International*, 1992, 859.
15. S. Yamamoto, B. Chang, Y. Kawano, R. Ozaki and Y. Murakami, ''Producing Spheroidal Graphite Cast Irons by Suspension of Gas Bubbles in Melts'', *AFS Trans.*, 1975, **83**, 217–226.
16. B. Chang, K. Akechi and K. Hanawa, ''*Spheroidal Graphite Iron*'', Agne Publish, 1983.
17. Y. Lee, ''*Action of Gas and Vaporised Element on the Change of Microstructure in Cast Irons*'', The Thesis of Doctor's Degree in Kyoto University, 1986.
18. Y. Kawano and T. Sawamoto, ''Production of Cast Iron with Fine Granular Graphite'', *AFS Trans.*, 1980, **88**, 463–470.
19. P. R. Khan, W. M. Su, H. S. Kim, J. W. Kang and J. F. Wallace, ''Effect of Filtration of the Melt by Different Ceramic Filters on Fluidity, Purity and Fatigue Strength of Spheroidal Graphite Cast Iron'', *Giessereiforschung*, 1988, **40**, 3, 101–109.
20. T. Ohide, ''Production of Iron Castings with Altered Graphite Morphology by a Modified in Mould Process', *Int. J. of Cast Metals Res.*, 1997, **9**, 279–284.

(Received 11 February 1999, accepted 7 February 2001)